Phosphorylation Modulates the Affinity of Light-Activated Rhodopsin for G Protein and Arrestin†

Scott K. Gibson, John H. Parkes, and Paul A. Liebman*

Department of Biochemistry and Biophysics, University of Pennsylvania Medical Center, Philadelphia, Pennsylvania 19104-6059

Received August 9, 1999; Revised Manuscript Received February 14, 2000

ABSTRACT: Reduced effector activity and binding of arrestin are widely accepted consequences of GPCR phosphorylation. However, the effect of receptor multiphosphorylation on G protein activation and arrestin binding parameters has not previously been quantitatively examined. We have found receptor phosphorylation to alter both G protein and arrestin binding constants for light-activated rhodopsin in proportion to phosphorylation stoichiometry. Rod disk membranes containing different average receptor phosphorylation stoichiometries were combined with G protein or arrestin, and titrated with a series of brief light flashes. Binding of G_t or arrestin to activated rhodopsin augmented the 390 nm MII optical absorption signal by stabilizing MII as MII·G or MII·Arr. The concentration of active arrestin or G_t and the binding constant of each to MII were determined using a nonlinear least-squares (Simplex) reaction model analysis of the titration data. The binding affinity of phosphorylated MII for G_t decreased while that for arrestin increased with each added phosphate. G_t binds more tightly to MII at phosphorylation levels less than or equal to two phosphates per rhodopsin; at higher phosphorylation levels, arrestin binding is favored. However, arrestin was found to bind much more slowly than G_t at all phosphorylation levels, perhaps allowing time for phosphorylation to gradually reduce receptor−G protein interaction before arrestin capping of rhodopsin. Sensitivity of the binding constants to ionic strength suggests that a strong membrane electrostatic component is involved in both the reduction of G_t binding and the increase of arrestin binding with increasing rhodopsin phosphorylation.

Activated G protein coupled receptors (GPCR) can catalyze GDP−GTP exchange on many G protein molecules, thereby amplifying signals relayed by agonists. The lifetime of an activated receptor must then be long enough to allow activation of a sufficient number of G proteins and effector molecules to elicit an appropriate cellular response. Equally important is the timing of termination and resetting of receptor activity to avoid overstimulation and to allow modulation of responses so that subsequent signals are interpreted in the appropriate context.

Many of the molecules and mechanisms of GPCR signal regulation were first discovered in the visual transduction pathway. This signaling pathway is initiated by photoisomerization of rhodopsin's covalently attached inverse agonist, 11-*cis*-retinal, to form *all-trans*-retinal, the agonist of rhodopsin interaction. Activated rhodopsin forms a long-lived equilibrium between two spectroscopically distinguishable intermediates, metarhodopsins I (λ_{max} 480 nm) and II (λ_{max} 387 nm; MI[1] and MII) (*1*). MII amplifies the signal by activating thousands of G proteins per second (*2*−*5*). The high MII catalytic activity coupled with its long natural lifetime (minutes) (*6*−*9*) requires MII activity to be rapidly quenched by additional receptor interactions (*10*) to prevent overstimulation and to maintain the fast time resolution of vision (<1 s).

Rhodopsin phosphorylation was found to be necessary for termination (quench) of the visual signal in vitro (*3*, *11*) and in vivo (*12*). The C-terminus of activated rhodopsin can be phosphorylated at multiple serines and threonines (*13*, *14*) by rhodopsin kinase (*15*). Rhodopsin phosphorylation reduces (*5*, *16*) or can completely block G_t activation under certain conditions (*17*). This effect is greatly enhanced by arrestin (*18*), which binds specifically to phosphorylated MII (*16*, *19*) and is thought to sterically occlude further G_t activation (*20*, *21*). In vivo studies have shown that receptor phosphorylation and arrestin binding are both required for normal deactivation of the visual signal (*22*).

Initial discoveries of the phosphorylation dependence of G_t activation and arrestin binding were carried out using a real-time assay of the activation of cGMP phosphodiesterase (PDE) that follows a weak light flash (*2*, *23*). Using this method, PDE activation was found to be diminished in

† Supported by NIH Grants EY00012, EY01583, and EY07035.

* Address correspondence to this author. Telephone: 215-898-6917. FAX: 215-573-8093. Email: liebmanp@mail.med.upenn.edu.

[1] Abbreviations: MI, metarhodopsin I; MII, metarhodopsin II; MIII, metarhodopsin III; RDM, rod disk membrane; OD, optical density; λ_{max}, maximum absorbance wavelength; PDE, cGMP phosphodiesterase; EDTA, ethylenediaminetetraacetic acid; NADPH, β-nicotinimide adenine dinucleotide phosphate, reduced form; DTT, dithiothreitol; K_{eq}, MI−MII equilibrium constant; G_t, retinal rod G protein (transducin); K_G, association constant of G_t for MII; K_R, association constant of arrestin for MII; R*, activated rhodopsin; K_d, dissociation constant.

10.1021/bi991857f CCC: $19.00
Published on Web 04/21/2000

proportion to phosphorylation stoichiometry in the absence of arrestin (*24*−*26*). Other work indirectly implied arrestin binding affinity to increase with phosphorylation stoichiometry (*25*). These observations are consistent with a function for multiple phosphorylation in regulating G protein activation, but the approaches used could not determine G_t binding constants or whether their magnitude was affected by the degree of MII phosphorylation.

In the absence of GTP or high concentrations of GDP, G_t binds MII, forming MII·G (*8*, *9*, *27*−*30*), the rhodopsin homologue of the GPCR high agonist-affinity state. This removes metarhodopsin in the form of MII·G from the MI−MII equilibrium (see reaction equations under Experimental Procedures), producing increased absorbance at 390 nm due to extra or enhanced MII formation (*9*, *27*). Since MII·G is spectroscopically identical to MII, its formation from MII is spectrally silent, the increase in 390 nm absorbance resulting only from that portion of the MII·G formed from MI. Similarly, arrestin binds and stabilizes highly phosphorylated MII as a MII−P·Arr complex (*19*) which is spectrally analogous to MII·G.

Parkes et al. (*31*) have developed a nonlinear least-squares fitting procedure (Simplex) that decouples the MI−MII equilibrium from the binding of G protein (or arrestin) to MII, using the increase in absorbance at 390 nm in response to each of a series of small bleaches. The procedure can determine a priori the initial concentrations of rhodopsin and activatable G_t, the MI−MII equilibrium constant (K_{eq}), the MII·G equilibrium constant (K_G), and the fraction of rhodopsin bleached by each flash, while calculating the amount of rhodopsin, MI, MII, MII·G, and free G protein at equilibrium after each flash. Using this approach, they determined that MII binds G protein (MII·G) on the RDM membrane surface with $K_G = (20-40) \times 10^3$ M^{-1} [solution equivalent $K_G = (2-4) \times 10^7$ M^{-1} or $1/K_G = 25-50$ nM].

Schleicher et al. (*19*) also used the 380 nm absorbance increase caused by MII·Arr formation to show that arrestin binds specifically to phosphorylated MII. Assumption of a 1:1 binding model led to a calculated K_d of 50 nM for MII·Arr at an average phosphorylation stoichiometry of 5.5−6.0 PO_4/Rh.

It has not previously been determined exactly how many of rhodopsin's C-terminal serines and threonines can, if phosphorylated, actually modulate G_t and arrestin binding, and whether binding stoichiometry or strength is a function of phosphorylation stoichiometry. In this study, we used the extra-MII assay coupled with Simplex analysis to address these questions by measuring the binding affinities of G_t and arrestin to MII as a function of increasing rhodopsin phosphorylation stoichiometry. The role of local electrostatics in modulating these binding events was explored, and their implication for the statistical control of single rhodopsin activation lifetimes at the absolute threshold of vision is discussed in this context.

EXPERIMENTAL PROCEDURES

Preparation of Rod Disk Membranes. Rod disk membranes (RDM) were purified from bovine eyes obtained from a local slaughterhouse (*2*). Rhodopsin concentration was determined from its absorption spectrum using the Dartnall correction for light scattering (*32*).

Preparation of Phosphorylated Rhodopsin. Rhodopsin samples with increasing average phosphorylation stoichiometries were produced as previously described (*33*). After phosphorylation, rhodopsin regeneration, and retinal reduction, RDM were hypotonically stripped to remove peripheral membrane proteins (*15*) and were finally resuspended in pH 7.0 10 mM KH_2PO_4, 25 mM KCl, 0.01 mM EDTA, and 1 mM DTT, at a stock concentration of about 200 μM.

Purification of Arrestin. Arrestin was prepared from fresh bovine retinas as described (*34*) and further purified by Sephacryl S-200 gel filtration (Pharmacia, Uppsala, Sweden). Fractions were concentrated to ∼200 μM and buffer-exchanged in pH 7.0 10 mM KH_2PO_4 with 50 mM KCl using Centricon C-30 (Amicon, Beverly, MA) spin concentrators. Arrestin concentration was determined by UV spectroscopy ($\epsilon_{280} = 23\,700$ M^{-1} cm^{-1}).

Purification of G Protein. $G_{\alpha\beta\gamma}$ was purified from fresh bovine retinas by the method of Baehr et al. (*35*). G_α and $G_{\beta\gamma}$ were separated and purified as previously described (*36*). All procedures were performed on ice or at 4 °C. Purification was completed in 2 days. Individual subunits were concentrated to ∼100 μM in Millipore Ultrafree-15 spin concentrators (Millipore, Bedford, MA) and buffer-exchanged to 10 mM KH_2PO_4, pH 7.0. Concentrations were determined by UV spectroscopy using $\epsilon_{280} = 36\,700$ M^{-1} cm^{-1} for G_α·GDP and 55 700 M^{-1} cm^{-1} for $G_{\beta\gamma}$ (*31*). All purified proteins were snap-frozen in 100 μL aliquots and stored in liquid nitrogen. Aliquots were rapidly thawed just before use.

Measurement of MII·G and MII·Arr Formation. An incremental bleaching method was used to measure G_t and arrestin through their binding to MII (*31*, *37*). A known concentration of either G_t (a stoichiometric combination of purified G_α and $G_{\beta\gamma}$) or arrestin was combined with RDM samples that had been pre-phosphorylated to average phosphorylation stoichiometries of 0.0, 1.1, 2.4, and 4.1 PO_4/Rh. These were then titrated with 39 light flashes of equal intensity produced by an EG&G Electrooptics (Salem, MA) xenon flash unit (FX-199 tube, PS-302 power supply set at 500 V, with a 7 μF external capacitor). The MI−MII equilibrium established after each flash was monitored by measuring the optical density at 390/426 nm with an SLM/Aminco DW2000 dual-wavelength spectrophotometer (Urbana, IL) equipped with a thermally jacketed cuvette holder connected to a constant-temperature water circulator. All measurements were made in quartz cuvettes with a 1 cm path length (measuring beam axis) and a width of 0.4 cm (bleaching axis). Each experimental sample contained approximately 9 μM rhodopsin, measured spectroscopically before each experiment, and either 0.6−0.8 μM G_t or arrestin. All experiments were performed at 10.0 °C.

About 2.5% of the remaining rhodopsin was bleached per flash. The period between flashes was extended in the first part of the flash series to allow sufficient time for the binding equilibrium to be established before the next flash was applied. As the free G_t or arrestin was exhausted, the interval between flashes was reduced. Intervals of 200 s separating the first three flashes were thus successively reduced to 150 s (flashes 4−6), 100 s (flashes 7−11), and 50 s (flashes 12−39).

Mathematical Analysis of G_t and Arrestin Binding to MII. Both G protein and arrestin bind to and stabilize MII (*9*, *19*) according to reaction Schemes 1 and 2. Determination of

Scheme 1

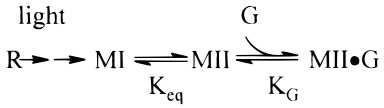

Scheme 2

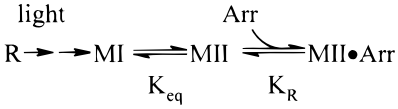

the equilibrium constants for enhanced MII formation requires two conservation and two equilibrium equations. The equations for arrestin enhancement are

$$[R^*] = [MI] + [MII] + [MII{\cdot}Arr] \quad (1)$$

$$[Arr]_{total} = [Arr]_{free} + [MII{\cdot}Arr] \quad (2)$$

$$K_{eq} = \frac{[MII]}{[MI]} \quad (3)$$

$$K_R = \frac{[MII{\cdot}Arr]}{[MII][Arr]_{free}} \quad (4)$$

The equations were solved for [MI], [MII], [MII·Arr], and $[Arr]_{free}$ as a function of the parameters $[Arr]_{total}$, K_{eq}, K_R, and *f*, the fraction bleached (*31*). The predicted change in optical density per flash is

$$\Delta OD = \Delta[R^*] \times \Delta\epsilon_{(Rh\rightarrow MI)} + (\Delta[MII] + \Delta[MII{\cdot}Arr]) \times \Delta\epsilon_{(MI\rightarrow MII)} \quad (5)$$

where Δ[R*], Δ[MII], and Δ[MII·Arr] are the concentrations of activated rhodopsin, MII, and MII·Arr formed per flash, and $\Delta\epsilon_{(Rh\rightarrow MI)}$ ($-7200\ M^{-1}\ cm^{-1}$) and $\Delta\epsilon_{(MI\rightarrow MII)}$ ($42\,000\ M^{-1}\ cm^{-1}$) are the Rh→MI and MI→MII differential extinction coefficients at 390/426 nm.

Dissociation of GDP after binding of G protein to MII involves an additional step, GDP release with reversible rebinding. But loss of GDP from G in the presence of R* is so complete in the absence of added GDP *(30)* that its reversal reaction and therefore the intermediate MII·G·GDP state need not be separately considered. This is consistent with the treatments of many previous studies *(8*, *9*, *18*, *19)*. Thus, the definition for K_G used here is the same as that for K_R and gives the correct total amount of MII·G formed and the amounts of free MII and G protein, so that the two binding constants are directly comparable *(31)*.

At 10.0 °C, the kinetic records showed a slow loss in $OD_{390nm} - OD_{426nm}$ due to formation of MIII from MII (for example, see Figure 1). The kinetic data were corrected for MIII formation as previously described (*33*), before use in subsequent equilibrium analysis. The correction removed any post-flash downward slope from the data. A Simplex algorithm was used with eqs 1−5 to generate values for K_{eq}, *f*, and the concentration of enhancing protein (either G_t or arrestin) with its binding constant to MII (K_G or K_R) that gave the best fit to the equilibrium data (*31*).

The same fitting procedure was used to determine the parameters for arrestin and G_t enhancement of MII, though the analyses differed in one respect. Interactions between rhodopsin and G_t occur on a membrane; therefore, Simplex analysis of MII enhancement by G_t fixed the initial rhodopsin concentration at its membrane concentration of 10 mM and calculated the corresponding membrane concentration of G_t to fit the data (*31*). After each iteration, the concentrations of rhodopsin and its bleaching intermediates were converted to their equivalent solution concentration and fitted to the OD measurements to give a solution-equivalent value for K_G. Since arrestin is a soluble protein, its solution concentration, together with the average solution concentration of rhodopsin, was used in the arrestin analysis. Only solution-equivalent binding constants are referred to in the discussion below.

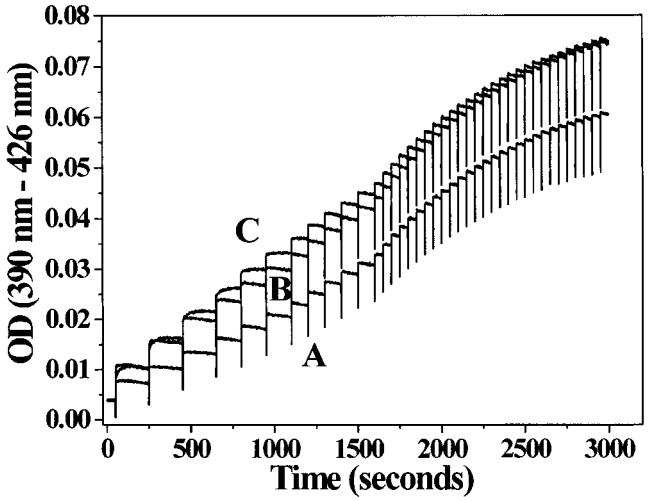

FIGURE 1: Examples of 39 flash MII enhancement assays for G_t and arrestin. 9 μM hypotonically stripped RDM alone (trace A), with 0.6 μM G_t added (trace B) or 0.6 μM arrestin added (trace C), was titrated with small increments of activated rhodopsin produced by brief light flashes. Each flash bleached approximately 2.5% of the remaining rhodopsin. Average phosphorylation stoichiometry was 2.4 PO_4/Rh. Measurements were performed at 10.0 °C, pH 7.5, with 100 mM KCl. Equal concentrations of G_t and arrestin are seen to produce the same increase in OD at the end point of the titration.

RESULTS

Phosphorylation Dependence of G Protein Binding Affinity. Figure 1 (trace B) shows that phosphorylated rhodopsin binds G_t and produces MII enhancement. Phosphorylation alone was previously found to increase the MI−MII equilibrium constant (*33*, *38*); therefore, the increase in MII that occurs in a flash titration series using different rhodopsin phosphorylation stoichiometries could not be directly compared without separately deconvolving the effect of phosphorylation on the two reactions. The Simplex nonlinear least-squares fitting procedure decouples these reactions (see Experimental Procedures). The resulting analysis showed G_t affinity for MII to decrease with increasing phosphorylation (Figure 2). The solution-equivalent MII·G affinity constant decreased from 65 μM^{-1} for unphosphorylated rhodopsin to 7.5 μM^{-1} at 4.1 PO_4/Rh. The actual affinity constants at local membrane concentration of reactants are about 1000-fold weaker than solution-equivalent values (*31*).

Phosphorylation Dependence of Arrestin Binding Affinity. Figure 1 (trace C) shows that arrestin binding to light-activated phosphorylated rhodopsin also stabilizes MII. Equal concentrations of arrestin or G_t are seen to stabilize equal

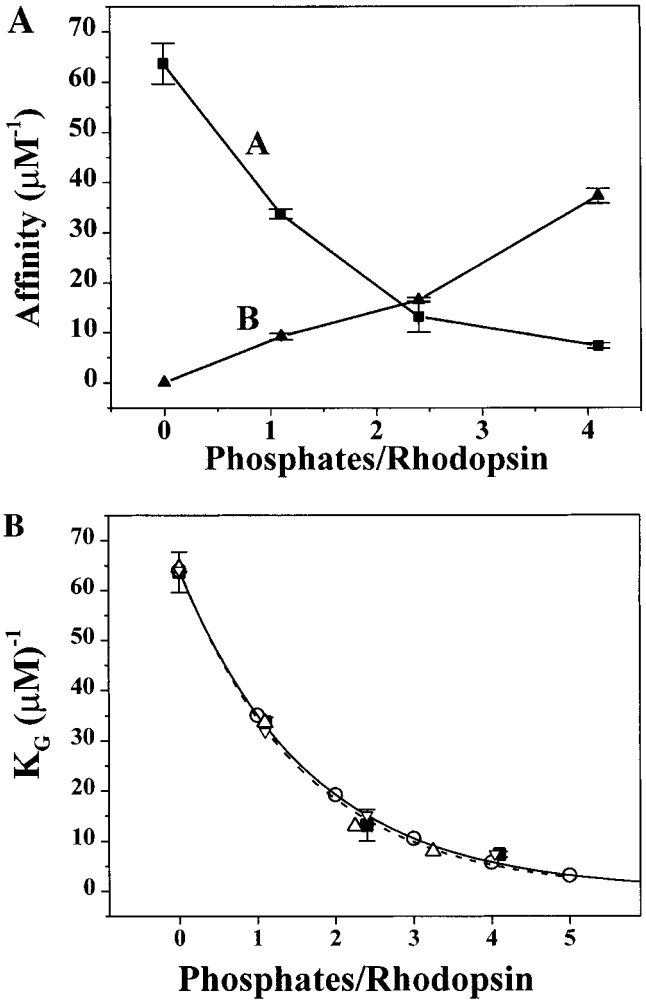

FIGURE 2: (A) Phosphorylation dependence of G_t (trace A) and arrestin (trace B) affinity for MII. Increasing rhodopsin phosphorylation decreases G_t affinity while increasing arrestin affinity. G_t binding is favored below 2.3 PO_4/Rh, while arrestin binding is favored above 2.3 PO_4/Rh. Measurements were made at pH 7.5, 100 mM ionic strength, and 10.0 °C. Each data point represents two or three experiments. (B) Apparent binding constants of G protein to rhodopsin at four average phosphorylation levels are shown as in panel A (□'s with error bars). Best-fitting K_Gs for a Poisson distribution truncated at 9 PO_4/R* are shown as downward triangles (▽). Individual K_Gs determined by this best fit are shown as open circles (○), connected by a solid line. If the Poisson distribution was truncated at 5 PO_4/R*s; the resulting best-fitting K_Gs are shown as upward triangles (△), plotted at their true average phosphorylation level. The exponential fit to the individual K_Gs determined for 5 PO_4/R*s is shown as a dashed line.

amounts of MII at bleach saturation. Since MII·G and MII·Arr are assumed to have the same spectroscopic properties as MII, they must have the same binding stoichiometry as well. Arrestin binding to unphosphorylated rhodopsin could not be detected, in agreement with previous studies (*19*, *39*).

Simplex analysis showed the affinity of arrestin for MII (K_R) to increase almost linearly with phosphorylation (Figure 2), rising from an undetectable level for unphosphorylated rhodopsin to 37 μM^{-1} at 4.1 PO_4/Rh. Assuming a 1:1 binding stoichiometry between MII and G_t, Parkes et al. (*31*) found Simplex analysis to accurately determine the concentration of ambient G_t through its stabilization of MII. Arrestin concentrations determined in the same way were in similarly good agreement with those measured by UV absorbance (data not shown), indicating that MII binding to arrestin is also well described by a 1:1 binding stoichiometry.

Arrestin and G_t affinities for MII were found to be oppositely affected by phosphorylation, the former increasing while the later decreased. Comparison of the G_t and arrestin binding isotherms (Figure 2A) shows that phosphorylation stoichiometries less than or equal to about 2 PO_4/Rh favor G_t binding, while higher stoichiometries favor arrestin binding.

Effect of Multiple Phosphorylation States on Apparent Binding Constant. Our Simplex data analysis algorithm was designed to deal with a single binding constant between MII and G protein or arrestin. While this model is appropriate for unphosphorylated membranes, we needed to reexamine its interpretation where a mixture of phosphorylation states with different binding constants was known to be present. Apart from the average phosphorylation level, we did not know what phosphorylation levels of rhodopsin were present, their relative amounts, or their individual binding constants to G protein. We therefore constructed sets of synthetic data where all of these were known, and which could then be analyzed by our Simplex program, and the results were compared with these known values and with the real data.

Since the apparent G protein binding constants were observed to fall off approximately exponentially with phosphorylation (Figure 2A), we assumed that the underlying individual binding constants behaved similarly. Four sets of data were therefore constructed, assuming the following: (1) average phosphorylation levels approximately matching those of the experimental data, (2) a Poisson distribution of individual phosphorylations generated for each average phosphorylation level, truncated at 5−9 phosphorylatable sites, renormalized, and the average phosphorylation level redetermined, (3) exponentially declining binding constants for each phosphorylation level that approximately matched the K_G data of Figure 2A, and (4) independent equilibria among MI, MII, and MII·G for each phosphorylation level from 0 through 9, with different K_Gs but the same K_{eq}, coupled only through their equilibria with a common pool of free G protein.

Self-consistent values for MI, MII, MII·G, and free G were determined for each phosphorylation level after each bleach. Each of these intermediates was summed over the different phosphorylation levels for each bleach, the resulting ODs were determined, and the results were analyzed by the Simplex program. The MII·G binding constant at zero phosphates and the ratio by which the binding constant decremented with each additional phosphate were then adjusted so that the K_Gs derived from the synthetic data best fit the apparent K_Gs of the experimental data. The former were found to lie on or very close to the exponential curve connecting the individual values (Figure 2B), so that the single K_G determined for a mixture effectively interpolated, at its average phosphorylation level, between the values of the individual binding constants.

Since higher phosphorylation states were both increasingly infrequent and more weakly binding to G protein, it made little difference in the analysis whether the upper phosphorylation limit was set at 5 or 9 PO_4/Rh, provided that the resulting K_Gs were plotted at their true average phosphorylation levels. Although the data were constructed to test the interpretation of K_G when determined from a mixture of rhodopsins with different phosphorylation levels, the fit to

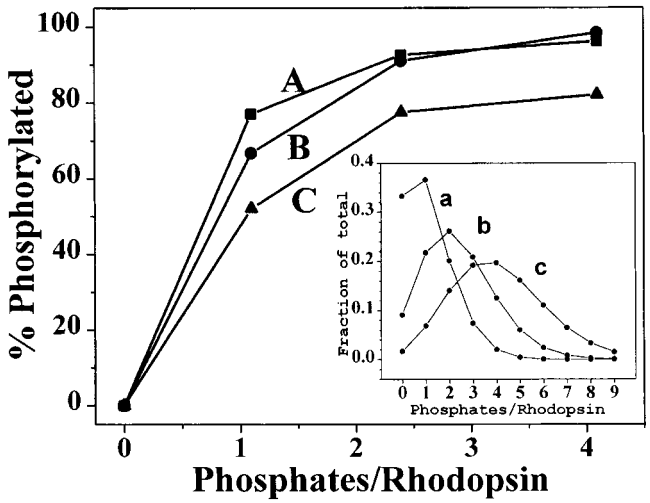

FIGURE 3: Percent of rhodopsin that contains at least one phosphate measured by MII·Arr formation (trace A), predicted by the Poisson distribution (trace B), and measured by Wilden and Kuhn (*14*) (trace C). Arrestin binds only phosphorylated rhodopsin; therefore, the amount of MII·Arr gives a lower limit for the percent of rhodopsin that is phosphorylated. The results show that phosphorylation is not cooperative, and that at 2.4 PO_4/Rh almost all rhodopsin is phosphorylated. Poisson distributions are shown (inset) for the three average phosphorylation levels.

the data is sufficiently good to suggest that there is some validity to the assumption of an exponential decrease in binding affinity to G protein with successive phosphorylations.

Determination of Fraction of Phosphorylated Rhodopsin. Some previous studies have suggested that rhodopsin phosphorylation might be cooperative (*14*, *40*, *41*). If this were true for our preparations, highly phosphorylated rhodopsins would contribute more strongly to the mean number of phosphates per rhodopsin than would be predicted by a Poisson distribution of phosphorylation numbers (see below). This could be interpreted to mean that the apparent rise in arrestin affinity with increasing average phosphorylation stoichiometry might be due simply to the increasing fraction of phosphorylated rhodopsins that exceed some critical stoichiometry, rather than to a more finely graded arrestin affinity increase with increasing phosphorylation.

It is known that only phosphorylated metarhodopsin can bind arrestin. Thus, MII·Arr formation can be used as a measure of the total amount of rhodopsin phosphorylated. Our Simplex analysis determines the exact amount of MII·Arr formed after each flash. The fraction of MII·Arr (plotted as a percent of total arrestin) formed from the first flash, where free arrestin is greatest, is plotted as a function of increasing phosphorylation in Figure 3. The plotted amounts are a lower limit for the percent of phosphorylated rhodopsin present, since activated phosphorylated rhodopsin would only be expected to form MII·Arr quantitatively if the product of $K_R \times [Arr] \gg 1$, i.e., very large K_R or very high arrestin concentration.

Cooperative rhodopsin phosphorylation implies formation of more copies of multiply phosphorylated rhodopsin than would be anticipated by the principle of phosphorylation independence. This would occur at the expense of the single phosphorylations for a given average. A Poisson distribution presumes each phosphate addition to be unaffected by previous phosphorylations; i.e., phosphorylation of an already phosphorylated rhodopsin is no more or less likely than phosphorylation of a previously unphosphorylated rhodopsin. For an average rhodopsin phosphorylation stoichiometry, *a*, the Poisson expectation of finding *n* phosphates per rhodopsin (fraction of molecules containing *n* phosphates) is given by

$$ {}_nP_a = \frac{a^n e^{-a}}{n!} $$

The probability that a bleached rhodopsin molecule contains one or more phosphates is one minus the probability that it has no phosphates. Thus, for our measured average of 1.1 PO_4/Rh:

$$ 1 - {}_0P_a = 1 - \frac{(1.1)^0 e^{-1.1}}{0!} = 1 - 0.33 = 0.67 $$

so that 67% of the bleached rhodopsins would be expected to have at least one phosphate in the absence of cooperativity. Truncating the Poisson distribution to a maximum of 9 PO_4/R* makes an insignificant error in this case.

We found 77% of bleached rhodopsin with this average level of phosphorylation to have formed MII·Arr on the first flash (Figure 3). This is higher than the Poisson estimate of 67%; higher also than the amount measured by Wilden and Kuhn (52%) (*14*). It suggests either that in the presence of phosphorylated rhodopsin, some unphosphorylated rhodopsin binds arrestin (this seems unlikely given that a completely unphosphorylated rhodopsin sample binds no arrestin), or that phosphorylation of rhodopsin is not cooperative.

Thus, the increase in arrestin affinity seen with increasing phosphorylation is not simply the result of an increased fraction of highly phosphorylated molecules. Maintaining the same average phosphorylation level would require more unphosphorylated rhodopsins, of which there are already too many to accurately fit the data. We can therefore conclude that rhodopsins with high phosphorylation stoichiometries do not accumulate to the early preferential exclusion of those of low phosphorylation stoichiometry. Rather, the data of Figure 3 can be explained as an incremental increase in K_R with each added phosphate.

Comparison of G Protein and Arrestin Binding Kinetics. Although the affinities of G_t and arrestin for MII are almost equal at 2.4 PO_4/Rh, their observed binding rate at equal concentration differs substantially. Kinetics of G_t binding to MII at 0.6 μM G_t are exponential with a relaxation time near 1 s under these conditions (Figure 4, trace A). Arrestin binding to MII at 0.6 μM arrestin is much slower, with a relaxation time of more than 20 s (Figure 4, trace B). Even at 4.1 PO_4/Rh, where arrestin affinity is 3-fold higher than that for G_t, phosphorylated rhodopsin formed MII·G_t much faster than it formed MII·Arr.

Ionic Strength Dependence of G Protein Binding Affinity. The C-terminus of rhodopsin, where all of its phosphorylation sites are located, is not required for G_t activation (*12*, *15*, *26*). Phosphorylation does not appear to affect the structure of rhodopsin in a way that intrinsically alters the MI−MII equilibrium. However, it does change the electrostatic character of rhodopsin and, through it, the membrane surface potential, membrane surface pH, and amount of MII formed (*38*). We investigated whether this change in local rhodopsin

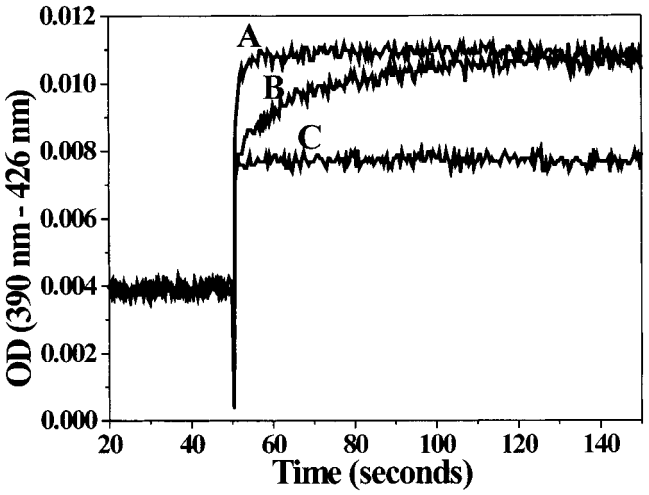

FIGURE 4: Kinetics of MII enhancement by G_t and arrestin. Response to the first flash of a titration series showing that arrestin binding (trace B) to MII with 2.4 PO_4/Rh is much slower than G_t binding (trace A). The lower curve (trace C) is the flash response of hypotonically stripped RDM with no MII enhancement. Measurements at 10.0 °C, pH 7.5, and 100 mM monovalent salt with 9 μM rhodopsin and 0.6 μM G_t or arrestin.

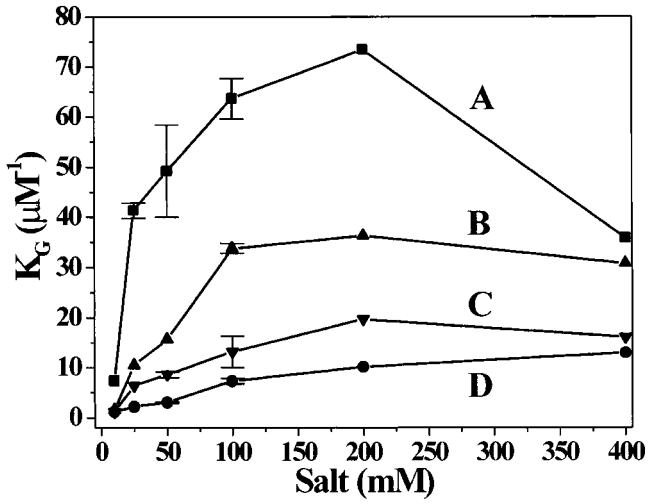

FIGURE 5: Ionic strength dependence of G_t affinity for MII at various phosphorylation levels. MII·G affinity increased with ionic strength from 10 to 200 mM for all phosphorylation stoichiometries: 0.0 PO_4/Rh (trace A), 1.1 PO_4/Rh (trace B), 2.4 PO_4/Rh (trace C), 4.1 PO_4/Rh (trace D). Increasing the ionic strength to 400 mM decreased G_t affinity for all phosphorylation stoichiometries except 4.1 PO_4/Rh, which showed a slight increase. Measurements were performed at pH 7.5 and 10.0 °C. Data points with error bars are the average of two experiments.

electrostatics might also account for the phosphorylation dependence of G_t binding.

To address this question, the ionic strength dependence of the MII·G interaction was determined. The binding affinity of G_t for MII increased with ionic strength from 10 to 200 mM KCl at all phosphorylation levels (Figure 5). However, further ionic strength increase from 200 to 400 mM KCl caused G_t binding affinity for unphosphorylated rhodopsin to decrease by about 50%. G_t affinity for 1.1 and 2.4 PO_4/Rh was also reduced, but only slightly. In contrast, G_t affinity for 4.1 PO_4/Rh continued to increase at high ionic strength.

The biphasic shape of the ionic strength dependence of G_t binding suggests that at least two effects on binding are being titrated: possibly membrane binding and binding to

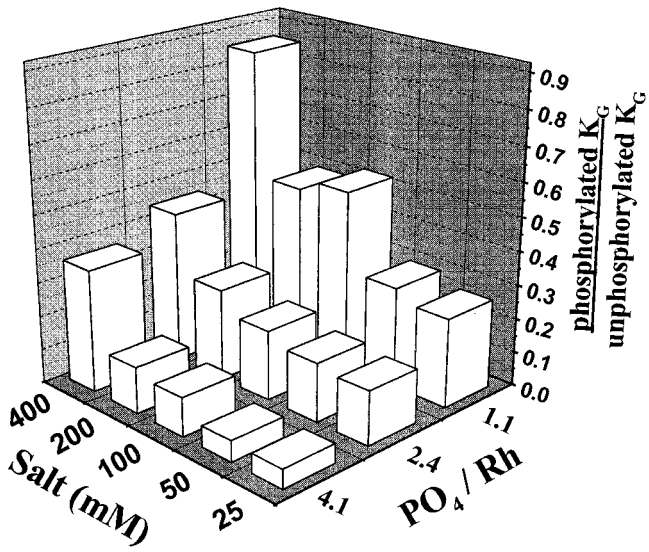

FIGURE 6: Ionic strength dependence of the K_G ratio of phosphorylated to unphosphorylated rhodopsin. The magnitude of the phosphorylation-dependent reduction in G_t affinity for rhodopsin is reduced with increasing ionic strength.

MII. Unlike other G proteins, G_t can be removed from the membrane at low ionic strength. Part of the reduction in G_t affinity at low ionic strength may thus be due to solubilization of G_t.

This effect is shown in Figure 6 as a plot of the ratio of K_G for phosphorylated rhodopsin to that for unphosphorylated rhodopsin as a function of ionic strength. The relative binding affinity of G_t for phosphorylated rhodopsin increases with increasing ionic strength at all phosphorylation levels. The data clearly show that phosphorylation-dependent reduction in MII·G affinity is augmented by low and attenuated by high ionic strength.

Ionic Strength Dependence of Arrestin Binding Affinity. Arrestin contains several sequences of contiguous cationic amino acids (*42*). Several of these form tertiary structural regions that are easily identified as positively charged patches on the X-ray crystal structure of arrestin (*43*, *44*). Such positive patches together with the increasing negative charge of rhodopsin upon phosphorylation suggest an electrostatic component to binding. The ionic strength dependence of arrestin binding to phosphorylated MII was therefore investigated to examine such electrostatic contributions.

The ionic strength dependence of MII·Arr affinity was found to be biphasic with maximum affinity near 50 mM ionic strength (Figure 7). As ionic strength increased beyond 50 mM, the MII·Arr affinity decreased. The association constant decreased from 44 μM^{-1} at 50 mM ionic strength to 7.6 μM^{-1} at 200 mM ionic strength for 4.1 PO_4/Rh. In addition, affinities of arrestin for all phosphorylation stoichiometries converged near 200 mM ionic strength. At ionic strength below 50 mM, K_R diminished at both 4.1 and 2.4 PO_4/Rh while K_R for 1.1 PO_4/Rh showed little change.

pH Dependence of G Protein Affinity for MII. Binding of G_t to MII is accompanied by the uptake of a proton (*45*). FTIR spectroscopy suggests that the protonation site is a carboxylate at the rhodopsin cytoplasmic interface (*46*). G_t binding and activation by unphosphorylated MII exhibits a bell-shaped pH dependence that is well fitted by the sum of two titration curves (*31*, *47*−*50*). We therefore examined

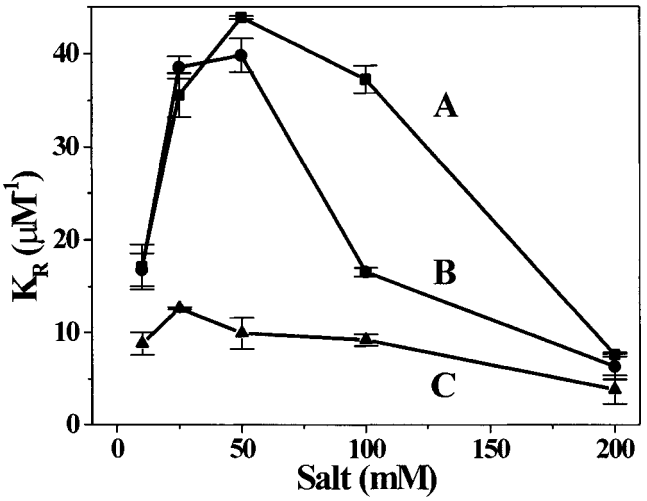

FIGURE 7: Ionic strength dependence of Arr affinity for MII at three levels of phosphorylation: 4.1 PO_4/Rh (trace A), 2.4 PO_4/Rh (trace B), and 1.1 PO_4/Rh (trace C). The affinity of MII for arrestin was maximal at 50 mM ionic strength and diminished at both lower and higher ionic strengths. Measurements were made at pH 7.5 and 10.0 °C. Data points with error bars are the average of two or three experiments.

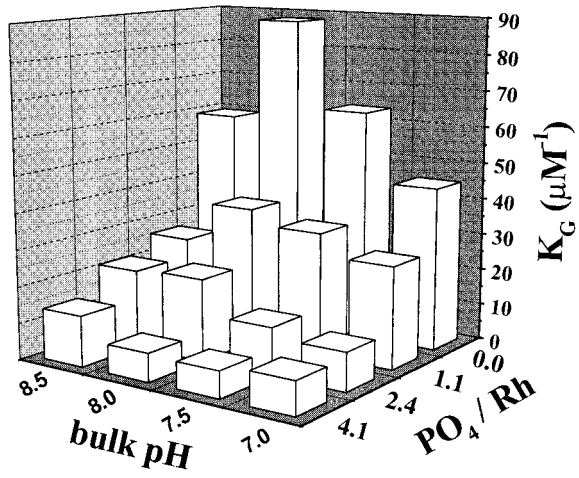

FIGURE 8: pH dependence of G affinity for MII at various phosphorylation levels. The biphasic pH dependence of G_t affinity is maintained at all phosphorylation stoichiometries. Maximum affinity shifts to more alkaline pH (very weak if at all) with increasing phosphorylation. Measurements were made at 10.0 °C in 100 mM monovalent salt.

the pH dependence of G_t binding to phosphorylated MII.

G_t binding affinity for unphosphorylated rhodopsin (K_G) was maximal near pH 8.0 (Figure 8), in agreement with previous studies (*31*). The pH dependence of G_t binding at 1.1 and 2.4 PO_4/Rh was also bell-shaped. The K_G maximum, however, shifted to more alkaline values with increasing phosphorylation stoichiometry. At 4.1 PO_4/Rh, the pH for maximum K_G was shifted beyond the range of our measurements to pH 8.5 or higher.

The phosphorylation-dependent shift in pH maximum for K_G may be attributed to changes in membrane surface pH. The Gouy−Chapman formulation described by Gibson et al. (*38*) was therefore used to calculate the membrane surface pH corresponding to each bulk pH. When the value of K_D at different phosphorylation levels is plotted as a function of bulk pH, the maxima appear to shift with pH. This shift largely disappears when plotted against membrane surface

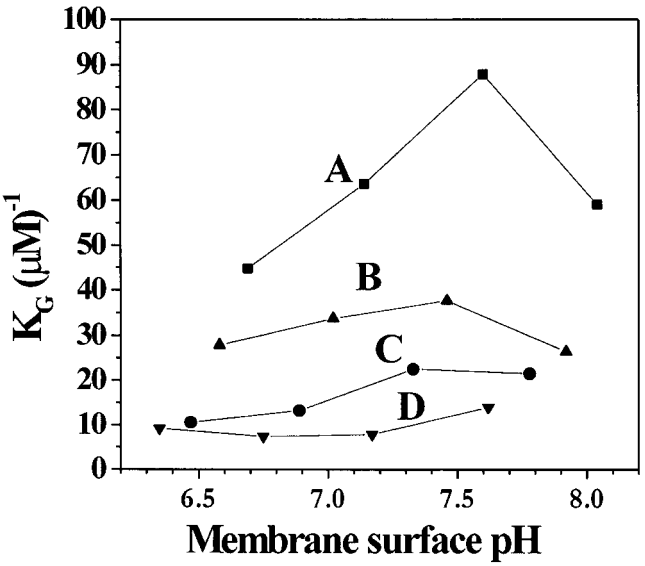

FIGURE 9: Membrane surface pH dependence of G protein affinity for MII at 0.0 PO_4/Rh (trace A), 1.1 PO_4/Rh (trace B), 2.4 PO_4/Rh (trace C), and 4.1 PO_4/Rh (trace D). The Gouy−Chapman equation *(38)* was used to calculate the membrane surface pH corresponding to each condition shown in Figure 8. This removes the effects of phosphorylation on the pH of maximum binding affinity. All phosphorylation stoichiometries have a K_G maximum near membrane pH 7.5. Points with error bars represent the average of two or three experiments.

pH. Like the MI/MII equilibrium itself, MII−G interaction depends on the membrane surface pH.

Enhanced OD at 390 nm is caused by formation of MII·G from MI. This limits the MII enhancement method for detection of G_t binding employed in this study to conditions where enough MI is initially present to allow an increase in 390 nm OD to be detected. Phosphorylation increases the apparent p*K* for MII formation (*33*, *38*) which makes K_{eq} too large (MI too small) for accurate measurements of MII enhancement below pH 7.0.

pH Dependence of Arrestin Affinity for Phosphorylated MII. The affinity of arrestin for MII increases more or less linearly with pH (Figure 10). K_R rises from 17.4 μM^{-1} at pH 7.0 to 77.5 μM^{-1} at pH 8.5 for 4.1 PO_4/Rh. Similar increases were found at 2.4 PO_4/Rh. The binding data for 1.1 PO_4/Rh also showed an increase in K_R with increasing pH, but the data fit became less accurate at pH 8.0 or above. With increasing pH or decreasing phosphorylation stoichiometry, the speed of arrestin binding decreased, so that the reaction did not reach equilibrium in the time between flashes. For example, the time constant determined from single-exponential fits of arrestin binding to 2.4 PO_4/Rh increased from 14 s at pH 7.0 to 31 s at pH 8.5.

The slow binding kinetics prevented accurate determination of K_R at pH levels higher than 8.5 for 4.1 PO_4/Rh and 2.4 PO_4/Rh. In addition, phosphorylation caused K_{eq} to become too large for accurate measurements of MII·Arr formation below pH 7.0 (*33*, *38*). Determination of the pH dependence of MII·Arr affinity was therefore limited to the relatively narrow range of pH 7.0 to pH 8.5. Nevertheless, the increased speed of arrestin binding with decreasing pH identifies another important action of rhodopsin phosphorylation that is mediated via its electrostatic effect on membrane surface pH.

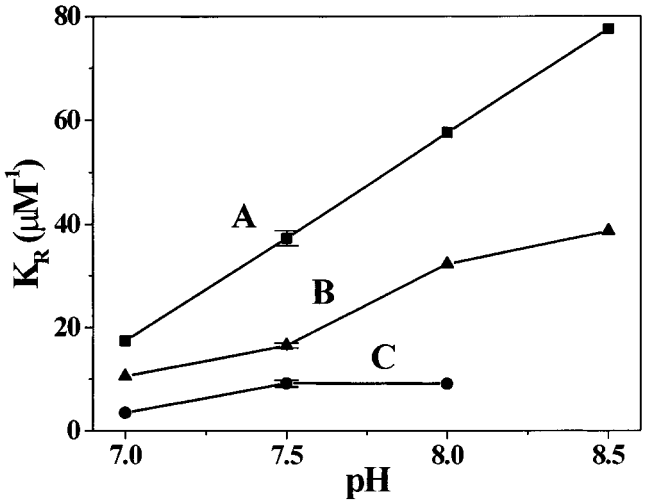

FIGURE 10: pH dependence of arrestin binding affinity for MII, measured at 4.1 PO_4/Rh (trace A), 2.4 PO_4/Rh (trace B), and 1.4 PO_4/Rh (trace C). Arrestin binding affinity increased linearly with increasing pH. The MI−MII equilibrium is shifted too far toward MII below pH 7.0 to obtain reliable data at the temperature of the experiments. At pH 8.5 and higher, the kinetics of arrestin binding were too slow to make reliable measurements for 1.1 PO_4/Rh. Measurements were made at 10.0 °C in 100 mM monovalent salt. Points with error bars represent the average of two or three experiments.

DISCUSSION

The early discovery that receptor phosphorylation terminates signaling activity (*3*) and lowers stimulus sensitivity in biochemical preparations of rod disk membranes (*10*) has been extended to many other GPCR systems (*51*). GPCRs contain a number of C-terminal serines and threonines that can be phosphorylated in vitro. Rhodopsin has nine such sites (*14*) while β2 and α2 adrenergic receptors have eight (*52*, *53*). The finding that phosphorylation stoichiometries greater than three phosphates per rhodopsin cannot be measured in vivo (*54*−*56*) seems to complicate this picture. Such studies suggest that in vitro conditions that allow more than these three phosphates to be incorporated are not representative of normal cellular rhodopsin quenching.

A possible difficulty in comparing in vitro with in vivo results is that in vivo phosphorylation determined by mass spectrometry required rather larger (10^{-4}) bleaches than might have been desirable since this intensity corresponds to multiple receptor activations per rod disk membrane. Sitaramayya and Liebman (*11*) showed that even after careful preservation of normal intracellular enzyme contents, bleaches of this magnitude produced much lower phosphorylation speed and stoichiometries than did weaker bleaches near 10^{-5}.

Weaker stoichiometries might be due to saturation of the small amount of available receptor kinase by an excessive amount of metarhodopsin substrate that decays to nonphosphorylatable opsin molecules before the saturated kinase can become available to phosphorylate them. Thus, it is still unclear how many of the several in vitro phosphorylation sites are relevant to in vivo modulation of G protein and arrestin binding at both single photon rod stimulation levels and those at higher light levels where relevant local conditions may change.

Though the present work does not examine low light intensities, it is important that both G protein and arrestin binding interactions with rhodopsin change with successive phosphorylations. These results may be of consequence both to the smoothing of single photon activation statistics and to the regulation of light sensitivity at higher light levels. Modulation of membrane electrostatics by rhodopsin phosphorylation may be an important part of these mechanisms.

Phosphorylation Simultaneously Modulates Arrestin and G_t Affinity for MII. We found that G_t affinity for MII was substantially reduced by increasing rhodopsin phosphorylation while, at the same time, arrestin affinity for MII was increased. The two binding curves crossed near 2.3 PO_4/Rh at pH 7.5 and 100 mM ionic strength. Were rod outer segment arrestin and G_t concentrations equal in vivo (*21*, *35*, *57*, *58*), arrestin binding would be expected to begin to dominate G_t binding at about 2−3 PO_4/Rh (in the absence of ambient guanine nucleotide). This is in the range of recent measurements that detected up to 3 PO_4/Rh in vivo following various light exposures (*54*, *55*).

Following light activation under intracellular nucleotide conditions (*59*), G_t is rapidly converted to G_α·GTP plus $G_{\beta\gamma}$ at a rate of ca. 2000 s^{-1} R^{*-1} (*5*), presumably depleting local membrane G_t concentration. Such a decrease in the local G_t to arrestin ratio might be expected to favor arrestin binding over G_t activation even at phosphorylation stoichiometries below 3 PO_4/Rh. However, this would clearly depend on the actual arrestin concentration in the rod outer segment under particular conditions of illumination. The majority of arrestin may be held in local inactive storage forms (*60*). The total concentration of arrestin has been found to increase from about 3 arrestins/100 rhodopsins in the dark to 10 arrestins/100 rhodopsins in room light through arrestin migration from the rod inner segment (*58*). At the same time, $G_{\beta\gamma}$ is lost from the membrane via binding to phosducin (*61*). G_α cannot bind RDM efficiently without $G_{\beta\gamma}$. More rapid GTP hydrolysis through binding of the GTPase accelerating protein (GAP) RGS9 may conversely return G_t to the membrane more rapidly. A balance between such competing effects is expected to influence the roles of phosphorylation and arrestin binding in quenching of activated rhodopsin.

Mechanism of Modulation by Phosphorylation. Electrostatic potential maps produced by the program GRASP (*62*) from the atomic coordinates of G_t (*63*) and arrestin (*43*) are shown in Figure 11. The region of arrestin postulated to bind rhodopsin is strongly positive (*43*, *44*) while the putative binding interface of G_t is mostly negative (*63*−*65*) with some small patches of positive potential. The oppositely charged rhodopsin binding surfaces of arrestin and G_t suggest an electrostatic mechanism that modulates binding through phosphorylation of MII. For G_t binding, the repulsive force that diminishes affinity between negatively charged phosphates and G_t should be abrogated by increasing ionic strength, resulting in stronger interaction. For arrestin binding, contributions to binding from interface countercharges should diminish with increasing ionic strength.

Phosphorylation-dependent decrease in MII·G affinity and increase in MII·Arr affinity were each found experimentally to be attenuated with increasing ionic strength, consistent with electrostatic modulation of these affinities by phosphorylation. The increased ionic strength would screen both negative phosphate charges and positive arrestin charges, thereby diminishing the electrostatic enhancement of phosphorylation on arrestin binding. The affinity of arrestin for

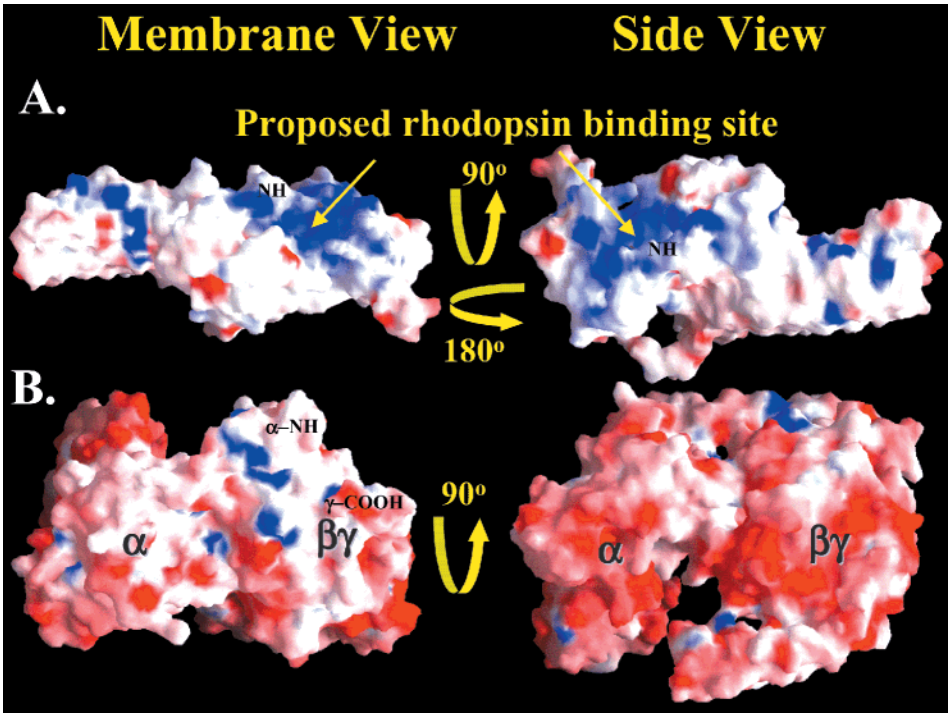

FIGURE 11: Electrostatic potential maps of arrestin (A) and G_t (B) were calculated using GRASP. The proposed rhodopsin binding site of arrestin has a strongly positive potential, which may interact with the negatively charged phosphates on rhodopsin's C-terminal tail. This interpretation is consistent with the phosphorylation stoichiometry, pH, and ionic strength dependence of arrestin binding affinity. G_t's putative RDM binding face is mostly negative, with some positive patches. The rest of the heterotrimer has a highly negative potential. The increase in negative charge on rhodopsin upon phosphorylation may electrostatically repel G_t, thereby explaining the phosphorylation-dependent decrease in G_t binding affinity. The ionic strength dependence of G_t affinity supports this hypothesis.

MII increases linearly with pH between pH 7.0 and 8.5 (Figure 5). The negative RDM surface potential also increases linearly within this pH range (*38*), consistent with an electrostatic mechanism.

Proteolytic (*15*, *26*) or mutational (*12*) deletion of rhodopsin's C-terminal tail has little effect on G_t activation. Phosphorylation of the C-tail might not be expected to affect G_t binding in a stereochemically specific way unless the tail position changes some specific interaction with rhodopsin's intradiskal loops. Such affinities are not known to be present (*66*). An NMR structure of the 19 amino acid peptide corresponding to the C-terminal tail of rhodopsin (residues 330−348) also showed little change in peptide conformation upon phosphorylation (*67*). On the other hand, a negative electrostatic potential produced by phosphorylation of rhodopsin's C-terminal tail could nonspecifically repel the negatively charged G_t binding surface, reducing MII·G binding affinity (see Figure 11). Rhodopsin phosphorylation has previously been shown to mediate other effects through its contribution to the disk membrane net negative surface charge and potential (*38*).

A model for the rhodopsin phosphorylation dependence of arrestin binding, based on the recent 2.8 Å crystal structure of arrestin and several mutational studies, has been proposed (*44*, *68*). The model suggests that the negative phosphate charge on rhodopsin's C-terminal tail destabilizes a series of salt bridges and hydrogen bonds between Arg-30, Arg-175, Lys-176, Asp-296, Asp-303, and Arg-382 in the polar core of arrestin. This region of arrestin has a strongly positive electrostatic potential which is thought to favor interaction with rhodopsin's phosphates. This interaction is proposed to cause arrestin conformational changes, releasing the initial constraints that prevent its binding to light-activated rhodopsin.

The above mechanism suggests how a single phosphate might electrostatically initiate arrestin binding. We have shown, however, that the affinity of MII for arrestin increases with each of several phosphorylations. The affinity of arrestin for inositol phosphates, which seems to mimic that for phosphorylated rhodopsin, also increases with degree of phosphorylation (*34*). It is unclear from previously proposed notions how multiple phosphorylation could enhance binding. Perhaps the stronger negative electrostatic field produced by multiple phosphates is more effective at disrupting the polar core of arrestin than a single phosphate. This is also consistent with the reduction in MII·Arr affinity at higher ionic strengths, which would shield the charges on arrestin and rhodopsin. Alternatively, a new model may be needed to explain the dependence of arrestin binding on the phosphorylation stoichiometry of rhodopsin.

Ionic strengths below 50 mM reduced K_R, apparently inconsistent with an electrostatic binding mechanism. However, the Debye length increase to >14 Å at these ionic strengths may allow more distant negative patches on arrestin to sense the potential and be repelled by the negatively charged RDM surface. Lowering the ionic strength from 50 to 10 mM also causes an approximately 0.5 unit decrease in membrane pH at 4.1 PO_4/Rh (*38*). Lowering the bulk pH from 7.5 to 7.0 reduces K_R approximately 2-fold (Figure 10). A portion of the drop in K_R at low ionic strengths may reflect this pH dependence. Alternatively, lower ionic strengths may strengthen electrostatic interactions within arrestin, making the bonds more difficult to disrupt.

Relevance to Molecular Mechanism of Reproducibility of Rod Single Photon Responses. Rod photoreceptors are remarkable for the unexpectedly high reproducibility of their electrical responses to single photons (*69*). This reproducibility is not consistent with a simple one-step molecular turnoff event of exponentially distributed lifetime like that preceding closure of an individual ligand-gated ion channel (*69*, *70*). Activated rhodopsin molecules are also expected a priori to have exponentially distributed lifetimes. Rods instead show intertrial single photon activation and recovery variation more characteristic of a 10−20 event averager (*70*). Though recent reconsideration may revise the estimated number of averaging events downward somewhat from 20 to near 7 (*71*), the measured low statistical variation in time to peak, duration, and integral charge carried suggests that R* activity is constrained to a duration that is nearly identical from trial to trial (*70*).

Light-activated rhodopsin (R*) is intrinsically long-lived (τ ca. 1 min). Liebman and Pugh (*3*) found ATP to allow much more rapid arrest of light activation of rod disk membrane phosphodiesterase via rhodopsin kinase-mediated phosphorylation (quenching) of rhodopsin, allowing only a brief window of rapid (2000 s^{-1}) G protein (*5*) and phosphodiesterase activation. Sitaramayya and Liebman (*15*) showed this quenching effect of ATP to be lost upon thermolysin proteolytic removal of rhodopsin's C-terminal dodecapeptide containing several of its phosphorylation sites. Quenching by ATP was thus found to act predominantly through the phosphorylation of sites from C-terminal to Thr-336 on rhodopsin. This result was more recently confirmed in vivo using a mouse rhodopsin C-terminal truncation mutant (*22*).

Sitaramayya and Liebman (*11*) also found that the rhodopsin phosphorylation associated with this quenching action was multiple and very rapid (>10 PO_4 per R* per second in vitro at 38 °C) at extremely weak bleaches that activated just 1 rhodopsin per disk or less (1.5×10^{-5} bleach). Higher bleach levels, even those as modest as 3×10^{-4}, yielded phosphorylation stoichiometries of 1 or less. Though seemingly low, a 3×10^{-4} bleach just saturates the rod disk PDE amplifier while the weaker bleach (1.5×10^{-5}) is in the linear range for this R*-mediated biochemical activation.

Using large bleaches, earlier workers mistook rhodopsin phosphorylation to be a slow process, both in vitro and in vivo (*72*, *73*). Sitaramayya and Liebman (*11*) found, however, that both the rate and stoichiometry of R* phosphorylation increase dramatically as bleaching is reduced to near 10^{-5}, where speed is no longer limited by excess R*. Our present work reinforces this view by showing that multiple phosphorylation is *not* processive; that is, a single kinase does not continue phosphorylation of a single rhodopsin to completion, to the exclusion of other bleached rhodopsins (Figure 3). Thus, the independence principle of a Poisson model appears consistent with our data over all phosphorylation levels. Together with the decay of many R*s before they can be phosphorylated, this result implies that even bleaches as weak as 10^{-4} might produce few bleached rhodopsins containing more than one phosphorylation.

Liebman et al. (*21*) speculated that successive phosphorylation events might serve to reduce the activity of an individual R* incrementally, each added phosphate reducing activity (ability to bind and activate G protein) by a fraction of its initial potency until zero activity was reached. Subsequent workers confirmed that R*'s ability to activate PDE is reduced with increasing rhodopsin phosphorylation stoichiometry (*24*−*26*). Figure 3 shows that antecedent MII·G interaction becomes progressively weakened by increasing phosphorylation, K_G decreasing about 2-fold per phosphate added. Decreased MII·G interaction would be the more proximal cause of reduced PDE activation. Evidence suggests that the speed of rhodopsin kinase would permit it to phosphorylate MII 3 or 4 times during the mean binding time of arrestin (*15*, *73*). The large difference between G protein and arrestin binding kinetics to rhodopsin (G protein being 2 orders of magnitude faster) may allow for gradual reduction in G protein activation through multiple phosphorylations of MII before arrestin can add its final, activity-terminating stochastic cap. R* activity would then be diminished in a series of small (receptor phosphorylation-dependent) steps that could smooth some of the variability of a single-molecule shutoff mechanism.

Upon discovery of the additional protein arrestin, it seemed possible that the activity-arresting effect of multiple phosphorylations might be mediated directly through a graded increase in arrestin binding affinity or dwell time (k_{off} decreasing) with increasing phosphorylation number, each arrestin binding event causing a rapidly reversible steric blockade of the receptor's G protein activation site. Increase in blocking duration was posited to continue to reduce activity until maximum phosphorylation was achieved.

In the present work, we *do* find that arrestin binding affinity increases almost linearly with rhodopsin phosphorylation stoichiometry. Were this arrestin binding initially weak with rapid dissociation and gradual buildup in affinity with phosphorylation as originally proposed (*21*), it might confirm the hypothesized intermittent R* blockage of gradually increasing duration through increasing phosphorylation stoichiometry. However, we find that the binding affinity of arrestin at even one phosphate per rhodopsin is already quite high at 10^7 M^{-1}. Together with the observed slow binding rate shown in the kinetic record of Figure 4, a flickering binding−dissociation with gradual blocking of R*'s access to G protein would not be possible as originally hypothesized. Given the observed binding affinity and on rate, the MII·Arr dissociation time is about 1000 s at 1 PO_4/R*. Thus, arrestin, once bound, would be sustained in the bound state for at least 15 min. These times would, of course, be faster at higher physiologic temperatures (*19*).

Schleicher et al. (*19*) determined a single arrestin K_d value of 50 nM at 5.5−6 PO_4/R*, in good agreement with our results (Figure 4). This high affinity for arrestin was compared to the weaker affinity for G protein at these high PO_4/R* ratios. These quantitative considerations confirm that arrestin binding contributes a final "capping" that prevents further G protein activation. It does not imply, however, that this effect actually *causes* the graded activity reduction that may precede it. Arrestin may *not* quench activation but simply maintain the quenched state. No subsequent studies have established affinity values for each phosphorylation state whose gradual increase could rationalize how increasing rhodopsin phosphorylation might explain both PDE activity reduction and the many-particle averaging character of electrophysiological uniformity of single photon responses.

G protein binding, even when weakened by phosphorylation, is much faster than arrestin binding (Figure 4). Thus, the ability of R* to interact with G protein is clearly reduced by phosphorylation in increments *before* arrestin has bound. This is due to rapidly reduced MII−G protein interaction through phosphorylation, rather than to competitive binding of arrestin. Thus, R* activity may be diminished in a series of small (receptor phosphorylation-dependent) steps that would smooth some of the variability of a single-molecule shutoff mechanism. It is possible that binding−dissociation stochastic cycles of rhodopsin kinase on the same time scale may further reduce the number of G binding events per second (*74*). These findings are consistent with other proposals that phosphorylation reduces PDE activation (*25*).

Based on data of the present study and others, we now propose that the ability of MII to bind and activate G_t is reduced in a series of steps of about 2-fold per phosphorylation. For optimal statistical averaging of several such successive phosphorylation steps, each step would need to dwell for an increasing duration such that the average product of each mean activity and duration was constant. Thus, if no one step were permitted to dominate, optimum statistical averaging of the ensemble of steps would be preserved. The much slower kinetics of arrestin binding together with its increasing speed and affinity with increasing phosphorylation might delay a single stochastic arrestin binding event until the ability of R* to activate G is so reduced by phosphorylation (50% at 1, 25% at 2, 12% at 3, 6% at 4 P/R*, etc.) that stochastic fluctuation in the exact moment of arrestin binding would matter little.

These smoothing events might then be augmented by others like the delayed onset of GTPase activity upon RGS9 binding and relaxation of the recoverin block of kinase activity, both activated cooperatively via the decrease in local Ca^{2+} concentration as cytoplasmic cGMP falls (*71*). Binding and dissociation of the kinase might further modulate this time-sharing cycle. Though such kinase binding has been called "pre-arrestin" (*74*), the combination of low kinase concentration and a low kinase on-rate constant would ensure that many G proteins continue to be activated between reversible kinase binding, phosphorylation, and kinase release cycles.

It has recently been reported that arrestin forms a stable dimer−tetramer equilibrium at cellular physiological protein concentrations (*60*). Our own measurements (data not shown) using dynamic light scattering confirm this observation. It is proposed that the arrestin oligomers might not themselves bind MII, but instead serve as a storage complex that releases low concentrations of arrestin monomers for rhodopsin binding as needed. An alternative view, however, is that the oligomers do bind phosphorylated rhodopsin, but more weakly and quickly (near their 100 μM concentration and at a rate near 100 s^{-1}) than the monomers. Thus, our earlier hypothesis of incremental rapidly reversible arrestin binding with increasing rhodopsin phosphorylation might still be a viable candidate for the source of statistical smoothing that accompanies rhodopsin quenching.

Whatever mechanics are involved, we believe the biochemical data indicate that R* interaction with G protein is always several hundredfold faster than it is with arrestin. This will allow considerable time before and during the several rhodopsin phosphorylations so that R*/G protein preamplifier gain (*3*) is reduced to near zero before arrestin adds its final activity-terminating stochastic cap. It will, of course, be necessary to extend the methodology described here and others to higher, near body temperatures, to appraise the physiologic relevance of these findings.

ACKNOWLEDGMENT

Robert Sharp provided technical assistance. We thank the NEI and Professor Rosalie Crouch for kindly providing 11-*cis*-retinal.

REFERENCES

1. Matthews, R. G., Hubbard, R., Brown, P. K., and Wald, G. (1963) *J. Gen. Physiol. 47*, 215−240.
2. Yee, R., and Liebman, P. A. (1978) *J. Biol. Chem. 253*, 8902−8909.
3. Liebman, P. A., and Pugh, E. N., Jr. (1979) *Vis. Res. 19*, 375−380.
4. Fung, B. K., and Stryer, L. (1980) *Proc. Natl. Acad. Sci. U.S.A. 77*, 2500−2504.
5. Liebman, P. A., and Pugh, E. N., Jr. (1982) *Vision Res. 22*, 1475−1480.
6. Ebrey, T. G. (1968) *Vision Res. 8*, 965−982.
7. Cone, R. A., and Cobbs, W. H. (1969) *Nature 221*, 820−822.
8. Bennett, N., Michel-Villaz, M., and Kuhn, H. (1982) *Eur. J. Biochem. 127*, 97−103.
9. Emeis, D., Kuhn, H., Reichert, J., and Hofmann, K. P. (1982) *FEBS Lett. 143*, 29−34.
10. Liebman, P. A., and Pugh, E. N., Jr. (1980) *Nature 287*, 734−736.
11. Sitaramayya, A., and Liebman, P. A. (1983) *J. Biol. Chem. 258*, 12106−12109.
12. Chen, J., Makino, C. L., Peachey, N. S., Baylor, D. A., and Simon, M. I. (1995) *Science 267*, 374−377.
13. Kuhn, H., and Dreyer, W. J. (1972) *FEBS Lett. 20*, 1−6.
14. Wilden, U., and Kuhn, H. (1982) *Biochemistry 21*, 3014−3022.
15. Sitaramayya, A., and Liebman, P. A. (1983) *J. Biol. Chem. 258*, 1205−1209.
16. Kuhn, H., Hall, S. W., and Wilden, U. (1984) *FEBS Lett. 176*, 473−478.
17. Sitaramayya, A. (1986) *Biochemistry 25*, 5460−5468.
18. Bennett, N., and Sitaramayya, A. (1988) *Biochemistry 27*, 1710−1715.
19. Schleicher, A., Kuhn, H., and Hofmann, K. P. (1989) *Biochemistry 28*, 1770−1775.
20. Wilden, U., Hall, S. W., and Kuhn, H. (1986) *Proc. Natl. Acad. Sci. U.S.A. 83*, 1174−1178.
21. Liebman, P. A., Parker, K. R., and Dratz, E. A. (1987) *Annu. Rev. Physiol. 49*, 765−791.
22. Xu, J., Dodd, R. L., Makino, C. L., Simon, M. I., Baylor, D. A., and Chen, J. (1997) *Nature 389*, 505−509.
23. Liebman, P. A., and Evanczuk, A. T. (1982) *Methods Enzymol. 81*, 532−542.
24. Miller, J. L., Fox, D. A., and Litman, B. J. (1986) *Biochemistry 25*, 4983−4988.
25. Wilden, U. (1995) *Biochemistry 34*, 1446−1454.
26. Miller, J. L., and Dratz, E. A. (1984) *Vision Res. 24*, 1509−1521.
27. Emeis, D., and Hofmann, K. P. (1981) *FEBS Lett. 136*, 201−207.
28. Kuhn, H., Bennett, N., Michel-Villaz, M., and Chabre, M. (1981) *Proc. Natl. Acad. Sci. U.S.A. 78*, 6873−6877.
29. Hofmann, K. P. (1985) *Biochim. Biophys. Acta 810*, 278−281.
30. Panico, J., Parkes, J. H., and Liebman, P. A. (1990) *J. Biol. Chem. 265*, 18922−18927.
31. Parkes, J. H., Gibson, S. K., and Liebman, P. A. (1999) *Biochemistry 38*, 6862−6878.
32. Knowles, A., and Dartnall, J. A. (1977) in *The Eye* (Davson, H., Ed.) pp 53−101, Academic Press, New York.

33. Gibson, S. K., Parkes, J. H., and Liebman, P. A. (1998) *Biochemistry 37*, 11393−11398.
34. Palczewski, K., Pulvermuller, A., Buczylko, J., Gutmann, C., and Hofmann, K. P. (1991) *FEBS Lett. 295*, 195−199.
35. Baehr, W., Morita, E. A., Swanson, R. J., and Applebury, M. L. (1982) *J. Biol. Chem. 257*, 6452−6460.
36. Kroll, S., Phillips, W. J., and Cerione, R. A. (1989) *J. Biol. Chem. 264*, 4490−4497.
37. Parkes, J. H., and Liebman, P. A. (1994) *Biophys. J. 66*, 80−88.
38. Gibson, S. K., Parkes, J. H., and Liebman, P. A. (1999) *Biochemistry 38*, 11103−11114.
39. Pulvermuller, A., Maretzki, D., Rudnicka-Nawrot, M., Smith, W. C., Palczewski, K., and Hofmann, K. P. (1997) *Biochemistry 36*, 9253−9260.
40. Aton, B. R., Litman, B. J., and Jackson, M. L. (1984) *Biochemistry 23*, 1737−1741.
41. Adamus, G., Arendt, A., Hargrave, P. A., Heyduk, T., and Palczewski, K. (1993) *Arch. Biochem. Biophys. 304*, 443−447.
42. Shinohara, T., Dietzschold, B., Craft, C. M., Wistow, G., Early, J. J., Donoso, L. A., Horwitz, J., and Tao, R. (1987) *Proc. Natl. Acad. Sci. U.S.A. 84*, 6975−6979.
43. Granzin, J., Wilden, U., Choe, H. W., Labahn, J., Krafft, B., and Buldt, G. (1998) *Nature 391*, 918−921.
44. Hirsch, J. A., Schubert, C., Gurevich, V. V., and Sigler, P. B. (1999) *Cell 97*, 257−269.
45. Schleicher, A., and Hofmann, K. P. (1985) *Z. Naturforsc., C: Biosci. 40*, 400−405.
46. Fahmy, K. (1998) *Biophys. J. 75*, 1306−1318.
47. Cohen, G. B., Oprian, D. D., and Robinson, P. R. (1992) *Biochemistry 31*, 12592−12601.
48. Fahmy, K., and Sakmar, T. P. (1993) *Biochemistry 32*, 7229−7236.
49. Surya, A., Foster, K. W., and Knox, B. E. (1995) *J. Biol. Chem. 270*, 5024−5031.
50. Kisselev, O. G., Meyer, C. K., Heck, M., Ernst, O. P., and Hofmann, K. P. (1999) *Proc. Natl. Acad. Sci. U.S.A. 96*, 4898−4903.
51. Lefkowitz, R. J. (1998) *J. Biol. Chem. 273*, 18677−18680.
52. Benovic, J. L., Regan, J. W., Matsui, H., Mayor, F. J., Cotecchia, S., Leeb, L., L. M., Caron, M. G., and Lefkowitz, R. J. (1987) *J. Biol. Chem. 262*, 17251−17253.
53. Benovic, J. L., Mayor, F. J., Staniszewski, C., Lefkowitz, R. J., and Caron, M. G. (1987) *J. Biol. Chem. 262*, 9026−9032.
54. Hurley, J. B., Spencer, M., and Niemi, G. A. (1998) *Vision Res. 38*, 1341−1352.
55. Chen, C. K., Burns, M. E., Spencer, M., Niemi, G. A., Chen, J., Hurley, J. B., Baylor, D. A., and Simon, M. I. (1999) *Proc. Natl. Acad. Sci. U.S.A. 96*, 3718−3722.
56. Ohguro, H., Van Hooser, J. P., Milam, A. H., and Palczewski, K. (1995) *J. Biol. Chem. 270*, 14259−14262.
57. Liebman, P. A., and Sitaramayya, A. (1984) *Adv. Cyclic Nucleotide Protein Phosphorylation Res. 17*, 215−225.
58. Philp, N. J., Chang, W., and Long, K. (1987) *FEBS Lett. 225*, 127−132.
59. George, J. S., and Hagins, W. A. (1983) *Nature 303*, 344−348.
60. Schubert, C., Hirsch, J. A., Gurevich, V. V., Engelman, D. M., Sigler, P. B., and Fleming, K. G. (1999) *J. Biol. Chem. 274*, 21186−21190.
61. Chen, F., and Lee, R. H. (1997) *Biochem. Biophys. Res. Commun. 233*, 370−374.
62. Nicholls, A., Sharp, K. A., and Honig, B. (1991) *Proteins: Struct., Funct., Genet. 11*, 281−296.
63. Lambright, D. G., Sondek, J., Bohm, A., Skiba, N. P., Hamm, H. E., and Sigler, P. B. (1996) *Nature 379*, 311−319.
64. Bourne, H. R. (1997) *Curr. Opin. Cell Biol. 9*, 134−142.
65. Hamm, H. E. (1998) *J. Biol. Chem. 273*, 669−672.
66. Cai, K., Klein-Seetharaman, J., Hwa, J., Hubbell, W. L., and Khorana, H. G. (1999) *Biochemistry 38*, 12893−12898.
67. Dorey, M., Hargrave, P. A., McDowell, J. H., Arendt, A., Vogt, T., Bhawsar, N., Albert, A. D., and Yeagle, P. L. (1999) *Biochim. Biophys. Acta 1416*, 217−224.
68. Vishnivetskiy, S. A., Paz, C. L., Schubert, C., Hirsch, J. A., Sigler, P. B., and Gurevich, V. V. (1999) *J. Biol. Chem. 274*, 11451−11454.
69. Baylor, D. A., Lamb, T. D., and Yau, K. W. (1979) *J. Physiol. 288*, 613−634.
70. Rieke, F., and Baylor, D. A. (1998) *Biophys. J. 75*, 1836−1857.
71. Whitlock, G. G., and Lamb, T. D. (1999) *Neuron 23*, 337−351.
72. Kuhn, H. (1974) *Nature 250*, 588−590.
73. Kuhn, H., McDowell, J. H., Leser, K. H., and Bader, S. (1977) *Biophys. Struct. Mech. 3*, 175−180.
74. Pulvermuller, A., Palczewski, K., and Hofmann, K. P. (1993) *Biochemistry 32*, 14082−14088.

BI991857F